8

Design and Evaluation of Self-Expanding Stents Suitable for Diverse Clinical Manifestation Based on Mechanical Engineering

Daisuke Yoshino and Masaaki Sato
Department of Biomedical Engineering, Graduate School of Biomedical Engineering,Tohoku University, Japan

1. Introduction

Atherosclerosis is one of the most prominent diseases that induce dysfunction of circulation, and it is a disease of large and medium size arteries. If cholesterol presenting at high concentration in a blood injures an intima, a white corpuscle, i.e. a monocyte, goes into the intima and mutates into a foam cell. Then, smooth muscle cells migrate from the media to the intima, and they grow proliferously there. Based on these phenomena, cholesterol and other lipid materials accumulate in the intima. Atherosclerosis has become a serious problem in the developed countries that are aging. Therefore, countermeasures to the atherosclerosis have become important. Although there are various medical treatments for the atherosclerosis, a stent placement has received much attention as a minimally invasive procedure for vascular stenotic lesion based on the coronary atherosclerosis, the arteriosclerosis obliterans, etc. A stent is a cylindrical tube-shaped medical device that can expand the stenotic lesion in a blood vessel continuously. When considering the expansion method of a stent, two types are available. One is a self-expanding type that can expand by itself when released from the sheath of a catheter. Another is a balloon-expandable type that must be expanded forcibly using a balloon catheter. Because the self-expanding stent continues to expand to the memorized diameter at the stenotic lesion, it has the long-term patency of a vascular wall. In the present study, the main target is the self-expanding type.

Recently, the severe problem of in-stent restenosis has arisen in a blood vessel with a stent placed and left in it. In-stent restenosis results from the neointimal thickening in the blood vessel based on the hyperplasia of smooth muscle cells. The hyperplasia of smooth muscle cells is caused by a mechanical stimulus from the stent to the vascular wall. The drug-eluting stent (DES) containing immunosuppressive agents is already in clinical use to resolve this problem (Morice et al., 2002). It can be said that the DES is more effective in preventing the development of restenosis than a bare metal stent (BMS). However, it can be said that the DES does not help to improve the life prognosis or to prevent myocardial infarction (Babapulle et al., 2004; Kastrati et al., 2007; Lagerqvist et al., 2007). It is also reported that the DES might cause deterioration in the life prognosis, although the BMS does not (Nordmann et al., 2006). Depletion of immunosuppressive agents has been pointed

out for longer use. When using a DES, such serious problem as side effects occurring by drugs must be considered as well. As described above, there have been many reports about the use of a DES to prevent in-stent restenosis. However, there have been few studies to prevent in-stent restenosis by designing and modifying a BMS itself. Most of studies have been undertaken to try improvement or optimization of the BMS. Shape, location, and mechanical properties of a stenotic lesion depend on each patient. Optimization, which derives one specified stent shape, is not always the best for the patient. It is thus necessary to design a stent shape suitable for each patient. Using a suitable stent can reduce the risk of in-stent restenosis. However, there has been no study that has tried to design a stent shape in response to each patient's symptom.

For providing a bare metal stent with lower risk of in-stent restenosis, two objectives were set up. The first objective of our research is establishment of a method to design a stent for each patient's symptom. The second objective is establishment of a method to select a suitable stent from commercially available stents based on their mechanical properties. In this chapter, we describe the design method and selection method of a stent suitable for patient's symptom based on mechanical engineering.

2. Method to select stent suitable for clinical manifestation based on evaluation of stent rigidities

It is important to evaluate mechanical properties of a stent for selecting one suitable for patient's condition. There have been many studies that have evaluated mechanical properties of a stent. (Duda et al., 2000) reported that the important properties of a stent include acceptable weight, stiffness in its radial direction, ease of insertion into the blood vessel, and radiation transmittance capability. They then proposed a method to evaluate stent and its performances. (Mori & Saito, 2005) performed a four-point bending test using a stainless steel stent to assess flexural rigidity for each different stent structure. (Carnelli et al., 2010) performed two mechanical tests on six kinds of carotid stents. They carried out a four-point bending test to assess flexibility of the stent. Their method of bending test was similar to that by (Mori & Saito, 2005). They also conducted a three-point compression test to measure the radial stiffness of the stent. Based on measurement results, they considered the relation between geometrical features of the stent and its mechanical properties. The results of these results provide a medical doctor the important information. If there exists a selection method of stent by using these evaluation results efficiently, the doctor can select a suitable stent easily in a large proportion of cases. However, there has been no study that has tried to propose the method to select a suitable stent by efficiently using evaluated mechanical properties. In this section, we introduce a method to select a stent suitable for patient's symptom based on mechanical properties of the stent.

2.1 Target stents

Four kinds of commercially available stents, which are already in clinical use, are evaluatedin addition to two types of SENDAI stents having different diameters. One of the evaluated stent is Protege® GPS™ (ev3 Endovascular, Inc., Plymouth, Minnesota, U.S.). The Protege® GPS™ has been developed for a bile duct. Zilver® (COOK MEDICAL Inc., Bloomington, Indiana, U.S.) and JOSTENT® SelfX (Abbott Vascular Devices, Redwood City, California, U.S.) are also biliary stents. Bard® Luminexx™(C. R. Bard, Inc., Murray Hill, New Jersey, U.S.) has been developed as a vascular stent. All six kinds of stents are self-

expanding stents made of NiTi shape memory alloy, namely Nitinol. Name, diameter, and length of each target stent are summarized in Table 1.

Stent	Code	Diameter (mm)	Length (mm)
SENDAI	SD10	10	80
Protege® GPS™ 10	GPS		80
Zilver®	ZIL		80
SENDAI	SD8	8	80
JOSTENT® SelfX	JSX		60
Bard® Luminexx™	BLU		100

Table 1. Dimensions of target stents

2.2 Radial compression test and stent stiffness in radial direction

The stent stiffness in radial direction was measured by using the radial compression test machine designed by reference to the method proposed by (Duda et al., 2000). A stent is mounted on the polytetrafluoroethylene stage with slit and wrapped in a sheet. As illustrated in Fig. 1, one end of the sheet is fixed, and the other end is pulled by the linear actuator (ESMC-A2; ORIENTAL MOTOR Co., LTD., Tokyo, Japan). By applying tensile force to the sheet, the stent is compressed in its radial direction. This tensile force can be measured by using the load cell (LUR-A-200NSA1, load rated capacity: 200 N; KYOWA ELECTRONIC INSTRUMENTS CO., LTD., Tokyo, Japan). In addition, the reduction of the stent diameter is measured by using the LED displacement sensor (Z4WV; OMRON Corporation, Tokyo, Japan). The sheet to wrap the stent consists of a polyethylene film 50 μm thick and a polyethylene terephthalate (PET) film 12 μm thick. Test temperature is 34 ˚C ± 1 ˚.

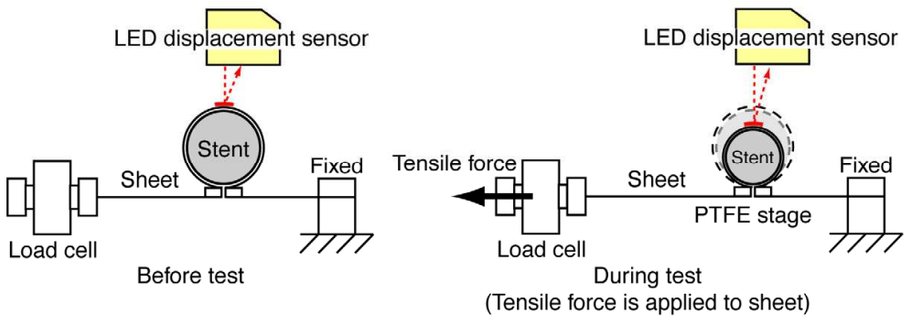

Fig. 1. Schematic view of the measuring method

(Duda et al., 2000) defined two kinds of forces for evaluating the scaffolding property of a self-expanding stent. One of the defined forces is chronic outward force, which is necessary to subtract 1 mm from a stent diameter. The other, namely radial resistive force, is needed to subtract 1 mm from a stent diameter. (Yoshino et al., 2008) defined the radial stiffness based on the radial pressure exerted on a stent for evaluating the scaffolding property. Based on these evaluation indicators, the stent stiffness in radial direction is defined as follows.

$$K_{p,f} = \frac{2\pi F}{\Delta r_s l_s} \tag{1}$$

Here, F is the tensile force measured by using load cell, l_s is the stent length, and Δr_s is the radius reduction of the stent.

The stent stiffness in radial direction was obtained from the measurement result by using equation (1). Figure 2 shows the comparison of the stent stiffness with each stent. For stent diameter of 10 mm, Protege® GPS™ has the highest stent stiffness in radial direction. On the other hand, for the stent diameter of 8 mm, the stent stiffness of Bard® Luminexx™ is the highest. Note that there is a difference of the stent stiffness in each stent.

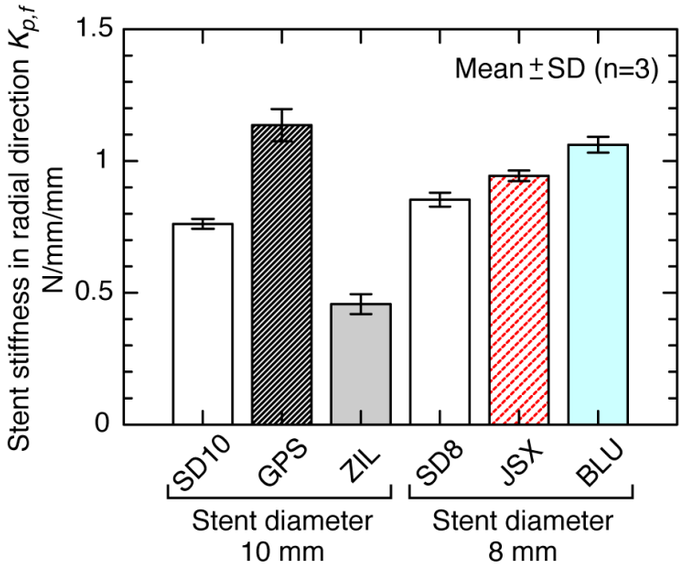

Fig. 2. Stent stiffness in radial direction of each target stent

2.3 Bending test and flexural rigidity

The flexural rigidity was measured by using the designed four-point bending test machine.

As illustrated in Fig. 3, stent is bent by using two pin indenters and a pair of support pins. The load to bend a stent and deflection of the stent are measured by using the micro load capacity load cell (LTS-1KA, load rated capacity: 10 N; KYOWA ELECTRONIC INSTRUMENTS CO., LTD.) and contact displacement transducers (Head: AT-110, Amplifier: AT-210, measurement range: ±5 mm, measuring force: 0.28 N; Keyence Corporation, Osaka, Japan). Here, the interval between support pins l_{sup} and that between pin indenters l_{ind} are set for 40 mm and 12 mm, respectively. In addition, the diameter of these pins is 3 mm. Test temperature is 35 ˚C ± 1˚.

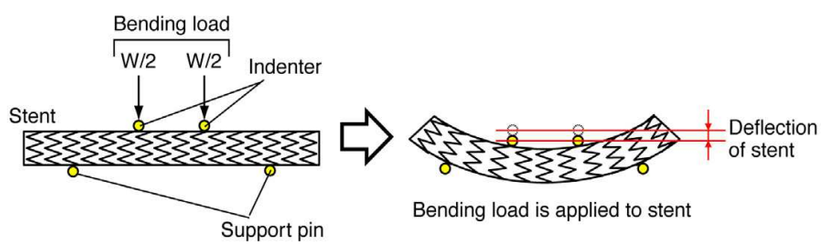

Fig. 3. Schematic view of the bending test

On the four-point bending test, shear force does not act on a stent between pin indenters. This enables us to apply a uniform bending moment to a stent. When considering the stent deformation as the problem of a simply supported beam, the differential equation of the deflection curve at the loading point is presented as follow.

$$\delta = \frac{\left(l_{\mathrm{sup}} + 2l_{\mathrm{ind}}\right)\left(l_{\mathrm{sup}} - l_{\mathrm{ind}}\right)^2}{48EI} W \tag{2}$$

Here, W is bending load. The product of Young's modulus E of the stent material and the moment of inertia of cross sectional area of the stent I exactly denotes the flexural rigidity K_b of the stent. Therefore, the flexural rigidity of the stent is derived from equation (2) as follow.

$$K_b = \frac{\left(l_{\mathrm{sup}} + 2l_{\mathrm{ind}}\right)\left(l_{\mathrm{sup}} - l_{\mathrm{ind}}\right)^2}{48} \frac{W}{\delta} \tag{3}$$

The flexural rigidity was obtained from measurement results by using equation (3). Figure 4 shows the comparison of the flexural rigidity with each stent. For the stent diameter of 10 mm, Protege® GPS™ has the highest flexural rigidity. On the other hand, the flexural rigidity of Bard® Luminexx™ is the highest in the stents with 8 mm diameter.

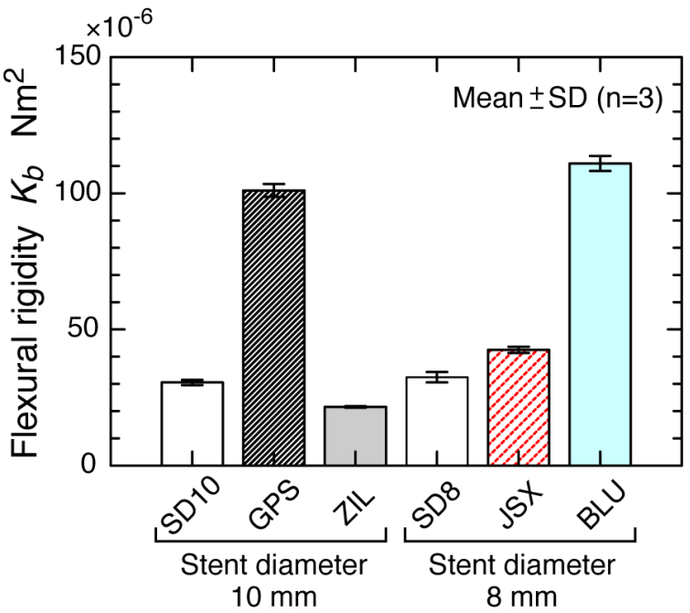

Fig. 4. Flexural rigidity of each target stent

2.4 Method to select stent suitable for clinical manifestation

Figure 5 shows flow of the proposed method to select a suitable stent based on mechanical properties. As preparation for selecting a suitable stent, the map of stent rigidity is made. The selection method is described below according to the flow illustrated in Fig. 5.

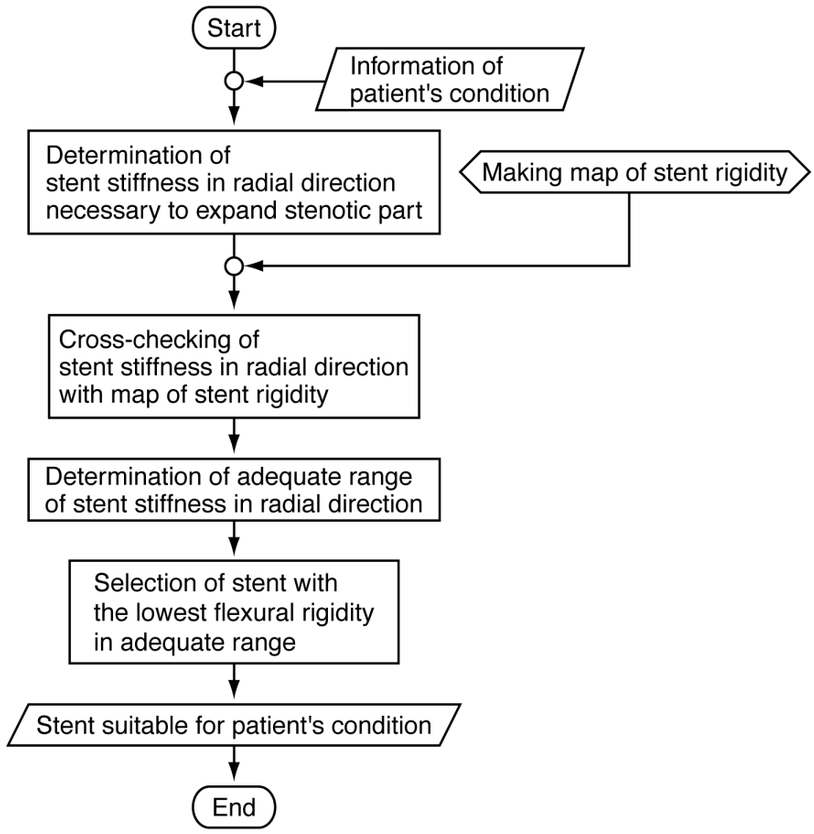

Fig. 5. Flow of selecting stent suitable for clinical manifestation

Step 1. Determination of stent stiffness in radial direction necessary to expand stenotic part: First, the stent stiffness in radial direction necessary to expand stenotic part is determined based on information of the patient's symptom. Requirements are the stent diameter d_s, the outer diameter D_o, the inner diameter D_i, and the least inner diameter D_l of the stenotic part. The pressure strain elastic modulus $E_{p,vl}$ of the diseased blood vessel is also needed. Other important information is the percentage by which to improve the blood flow level, namely the target diameter D_t after treatment. Given all the values listed above, the necessary radial stiffness can be obtained by the following equation (see in Section 6 for details).

$$K_p^* = 2E_{p,vl}\frac{D_t - D_l}{D_o\left(d_s - D_t\right)} \tag{4}$$

Equation (4) is derived from the radial pressure necessary to expand the stenotic part in the blood vessel. In this chapter, the radial force necessary to expand the stenotic part is considered as a standard. Therefore, K_p^* of equation (4) is converted into the necessary stent stiffness $K_{p,f}^*$ using the circumferential length of the vascular inside wall after treatment as follow.

$$K_{p,f}^* = 2\pi E_{p,vl}\frac{D_t\left(D_t - D_l\right)}{D_o\left(d_s - D_t\right)} \tag{5}$$

With the symptom information assumed as shown in Table 2, the necessary stent stiffness $K_{p,f}^*$ can be calculated using equation (5) as $K_{p,f}^*$ = 0.87 N/mm/mm (d_s = 8 mm), and $K_{p,f}^*$ = 0.48 N/mm/mm (d_s = 10 mm).

Artery	Carotid artery
Outer diameter, D_o (mm)	6.82
Inner diameter, D_i (mm)	5.60
The least inner diameter of stenotic part, D_l (mm)	2.80
Rate of stenosis by ECTS method (%)	50
Pressure strain elastic modulus of diseased artery $E_{p,vl}$ (MPa)	0.145
Target inner diameter after treatment, D_t (mm)	5.60

Table 2. Information of symptom assumed for selecting of stent

Step 2. Cross-checking of stent stiffness in radial direction with map of stent rigidity: The calculated $K_{p,f}^*$ values are plotted onto the map of stent rigidity, and indicated by broken lines presented in Fig. 6. It is difficult that the stent stiffness of a commercially available stent matches the calculated $K_{p,f}^*$ value.

Step 3. Determination of adequate range of stent stiffness in radial direction: As described above, there exist few stents that have the stent stiffness value equal to the calculated $K_{p,f}^*$ value. Therefore, the necessary stent stiffness $K_{p,f}^*$ is widened to the extent adequate to expand the stenotic part in the blood vessel. The doctor should normally determine this adequate range of the stent stiffness. In this case, it is determined that the range of ±10 % for the necessary stent stiffness $K_{p,f}^*$ is adequate. The shaded areas shown in Fig. 6 are the setup adequate ranges.

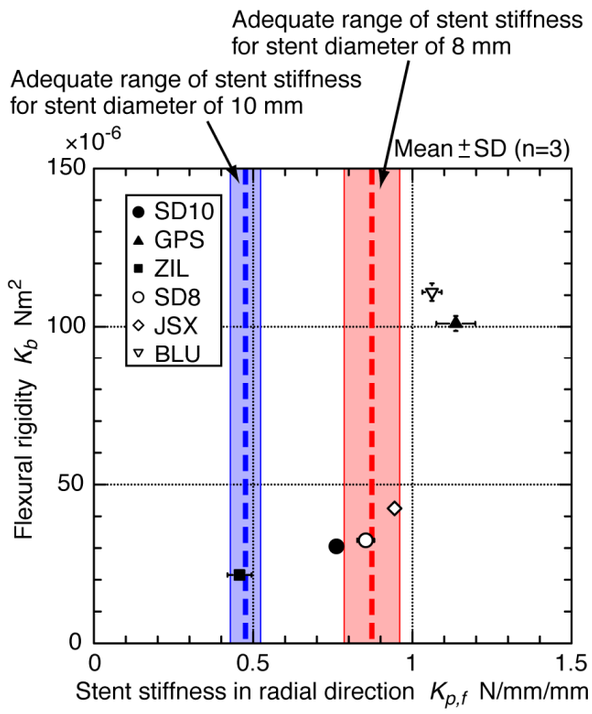

Fig. 6. Selection of suitable stent using map of stent rigidity

Step 4. Selection of stent with the lowest flexural rigidity in adequate range: If the stent, which is in the adequate range, is selected, it can expand the stenotic part in the blood vessel sufficiently. The stent sometimes has too high flexural rigidity for the lesion because of selection only in terms of the stent stiffness in radial direction. When selecting a stent, its flexural rigidity should be considered. But we have no basis of the flexural rigidity for selecting a stent. Therefore, it is decided to select the stent that has the lower flexural rigidity than any other stent being in the adequate range. For the assumed symptom, SENDAI (SD8, d_s = 8 mm) and Zilver® (ZIL, d_s = 10 mm) are most suitable.

In this section, we introduced the method to select a stent suitable for the patient's symptom based on mechanical properties of the stent. It is considered that the selection method can help doctors greatly in clinical sites. Commercially available stents are targeted for this selection method. There are limitations to selecting a suitable stent using this method. Therefore, a novel stent has to be designed for providing the stent more suitable for the patient's symptom. The method to design more suitable stent will be described in the following sections.

3. Design support system for self-expanding stents

A design support system for a self-expanding stent using CAD and CAE is introduced in this section. This support system can improve the efficiency of the suitable stent design.

3.1 Design variables of SENDAI stent

Figure 7 shows a two-dimensional diagram of a SENDAI stent. Each wire section is constructed from 12 loosely curved S-shaped wires. The strut section of the stent connects them using three bridge wires. On the two-dimensional shape of the SENDAI stent in Fig. 7, the design variables that might affect the mechanical properties of the stent are set. Here, l_w and l_b are the length of the wire and the bridge wire along the axial direction, θ_w and θ_b are the angle of the wire and the bridge wire to the axial direction, t_w and t_b are line element width of the wire and the bridge wire, and r_i and r_o are the inner radius and the outer radius of the wire end part. Every wire is structured in an arc shape. When the design variables l_w, θ_w, and others are given, the arc shape is determined and wire section is constructed through laying out these arc shapes continuously. Furthermore, the number of wires n_w, the number of bridge wires n_b, and the thickness of the tube material t_s are also design variables.

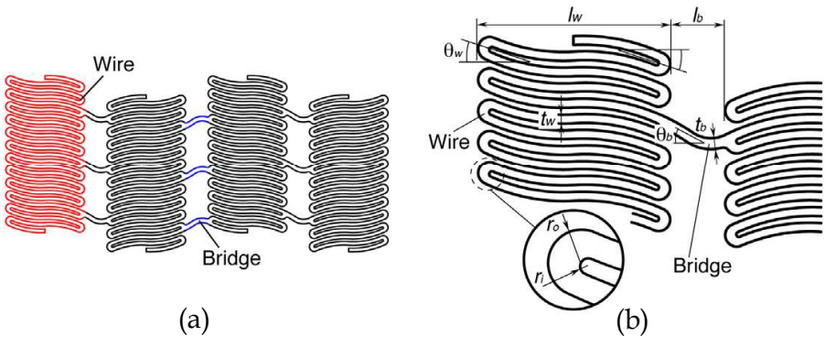

Fig. 7. Two-dimensional diagram of SENDAI stent (a) and main design variables for SENDAI stent (b)

3.2 Framework of design support system

Figure 8 shows the design support system for a self-expanding stent. The left-hand side of the figure shows the production process of the SENDAI stent. It has three production stages: a 'manufacture' stage, during which the NC data are created based on the two-dimensional diagram to manufacture the initial stent shape while the initial stent is manufactured by using laser processing; an 'expansion' stage, during which the initial stent is forcibly expanded in the radial direction by inserting a tapered rod into the stent as it is given shape-memory treatment; and an 'evaluation' stage, during which the performance of the expanded stent is tested. The right-hand side of Fig. 8 shows the flow of the shape design for self-expanding stents being proposed. A three-dimensional model of the initial stent manufactured by using laser processing is created from the two-dimensional shape by using 3D CAD. Then, by dividing into finite elements, the finite element model representing the initial stent is created based on the 3D CAD model, and the expanded stent shape is predicted by applying an expansion analysis using the finite element method for large deformation. Based on this prediction, a rigidity analysis is conducted using a non-linear finite element method. The mechanical properties of the stent are evaluated from the results. This process corresponds to the actual production process of the 'manufacture,' 'expansion,' and 'evaluation' stages.

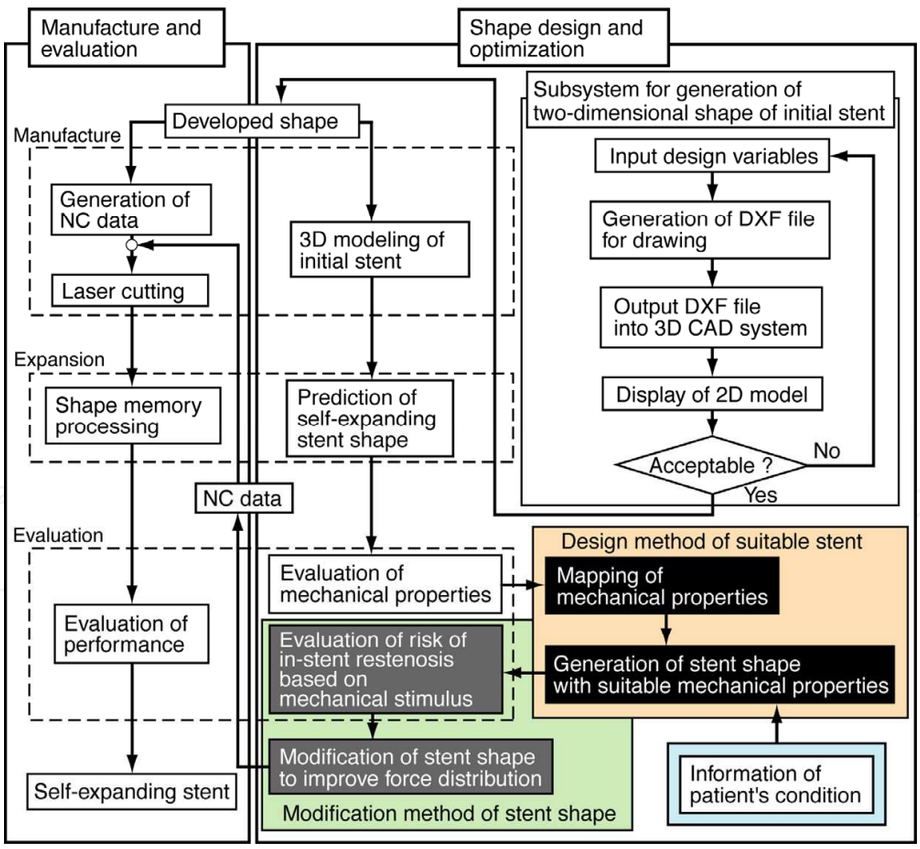

Fig. 8. Design support system for self-expanding stent. The left-hand side shows the production process of the SENDAI stent. The right-hand side shows the flow of the proposed design support system.

This support system has design method of a self-expanding stent suitable for the patient's symptom based on mechanical properties of a stent. This method is available to introduce into the existing design support system described above, and has two stages which are the design and modification methods. In the first stage, a stent shape with mechanical properties suitable for the patient's symptom is determined and designed. In the second stage, to modify the stent shape in consideration of the risk of in-stent restenosis realizes designing the stent shape more suitable for the patient's symptom. The risk of in-stent restenosis is evaluated based on a mechanical stimulus to a vascular wall by insertion of a stent. These two stages of the design method will hereinafter be described in more detail (see in Section 6).

After the two-stage design method, the design support system ends with the generation of the NC data of the designed stent necessary for moving onto the actual production process. For change in a stent shape, a subsystem for generating the two-dimensional shape of the initial stent was introduced, and this is available for changing the two-dimensional shape flexibly. It can also be used to generate a two-dimensional diagram of the stent in the first place.

4. Mechanical properties of stent

It is important to obtain sensitivities of mechanical properties of a stent to design variables when designing the stent suitable for patient's symptom. In this section, important mechanical properties, namely, radial stiffness, flexural rigidity, and shear rigidity, are evaluated and the maps of their sensitivities are made. The expanded stent shape is used for evaluation of mechanical properties. The expanded shape is predicted from the expansion analysis (see in (Yoshino & Inoue, 2010) for details).

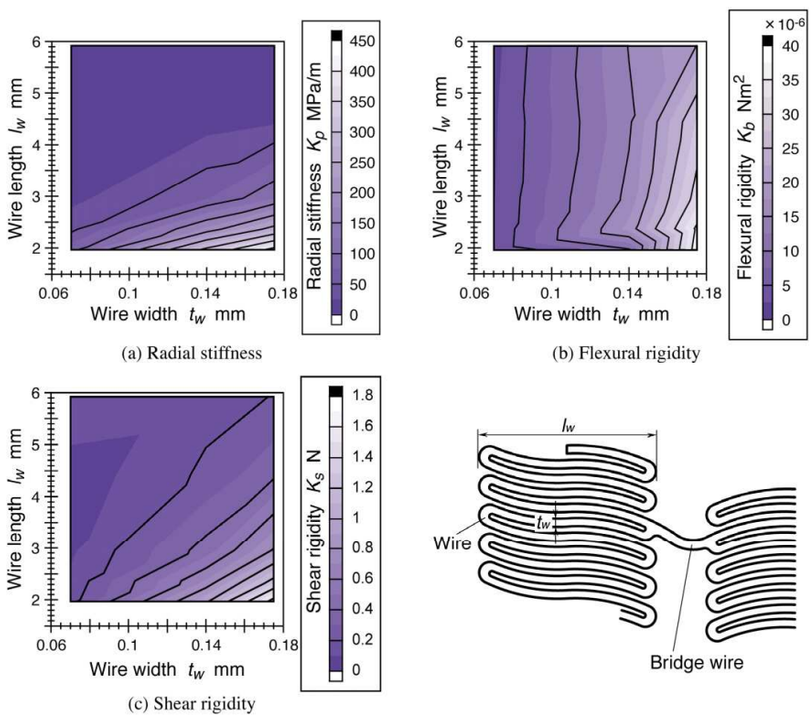

Fig. 9. Sensitivities of the mechanical properties of the SENDAI stent 6 mm diameter to thedesign variables: (a) radial stiffness, (b) flexural rigidity, and (c) shear rigidity

We must know the relationship between the mechanical properties of a stent and the design variables in order to design a stent with specific properties. The mechanical properties of the SENDAI stent, such as radial stiffness, flexural rigidity, and shear rigidity, were evaluated, and their sensitivities to the design variables were also defined, as shown in Fig. 9 (Yoshino & Inoue, 2010). The wire length along the axial direction and the wire width were selected as design variables. Isolines on the maps of mechanical properties are very important for proposing designs. The isoline is plotted onto the maps based on the required mechanical property, and design variables of the proposed design are determined from the isoline. In addition, we assumed the mechanical properties of the stent material as illustrated in Fig. 10: Young's modulus of 28 GPa, and Poisson's ratio of 0.3.

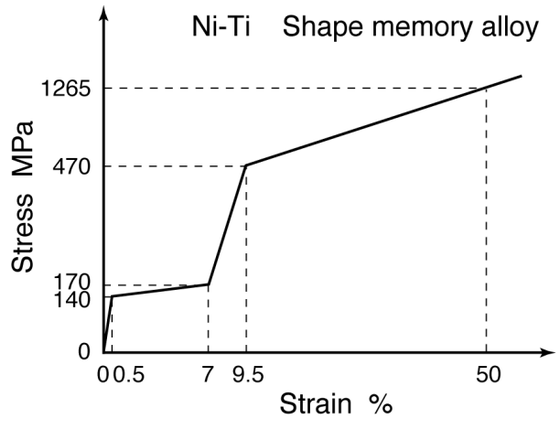

Fig. 10. Assumed stress-strain relationship for the stent material

5. Estimation of force on vascular wall caused by insertion of self-expanding stent

The forces on a blood vessel are classified into two categories: internal pressure caused by the expansion of the stent and the force resulting from the straightening of the blood vessel, which is a phenomenon whereby a curved blood vessel is straightened by the stent. Straightening of blood vessels often occurs in cases involving the use of a closed-cell stent. As a result, a problem occurs in that the straightening easily encourages kinking of the blood vessel at the flexural area distant from the stented lesion (Tamakawa et al., 2008).

In this section, focusing on a method by which to improve the force distribution on the vascular wall according to the symptoms of the patient, we introduce a method to compute the distribution of the contact force between the stent and the blood vessel under the assumption that the stent is inserted into a straight blood vessel. In the method, the stent and the blood vessel are simplified as axisymmetrical models. Then a method for calculating the distribution of the straightening force on the vascular wall is introduced.

5.1 Computation of contact force distribution on vascular wall caused by expansion of stents

The expansion of a stent in a blood vessel induces pressure on the contact surfaces of the stent and the blood vessel. Analysis of pressure or contact force based on the complicated

shape of stent is a difficult and time-consuming task. Therefore, a simplified calculation method using the axisymmetrical models is presented as shown in Fig. 11. The stent is modeled by a number of rings, indicated by broken lines in Fig. 11. The wire section is represented by 11 rings. The blood vessel is similarly modeled by rings, where the ring intervals are the same as those of the stent. In addition, it is assumed that the blood vessel is much longer than the stent. It is also assumed that these rings deform axisymmetrically due to the uniformly distributed radial force.

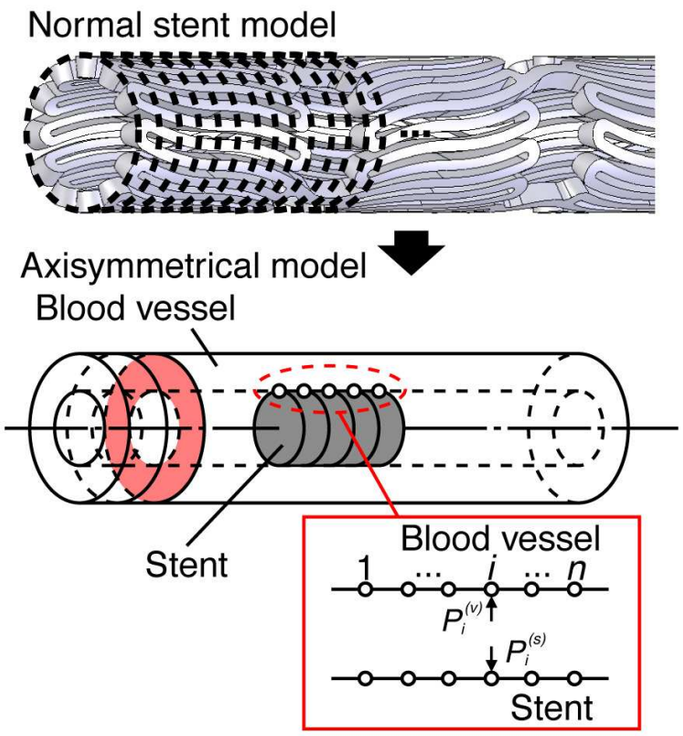

Fig. 11. Model used to compute the contact force between the stent and vascular wall. Thestent and blood vessel are simplified to axisymmetrical models.

Next, let us consider ring i (i = 1, 2, ..., n) in contact along the surfaces of stent and vascular wall. When a unit radial force is applied to ring i of model m (m = s, v, which correspond to the stent and the blood vessel, respectively), the radial displacement at ring j, denoted as $r_{ji}^{(m)}$, is calculated using the finite element method. The influence matrix $[C^{(m)}]$ is defined in terms of as $r_{ji}^{(m)}$ as follows:

$$\left[C^{(m)}\right] = \left[\left\{r_1^{(m)}\right\}, \left\{r_2^{(m)}\right\}, \ldots, \left\{r_n^{(m)}\right\}\right] \tag{6}$$

where

$$\left\{r_i^{(m)}\right\} = \left(r_{1i}^{(m)}, r_{2i}^{(m)}, \ldots, r_{ni}^{(m)}\right)^{\mathrm{T}} \tag{7}$$

The radial displacement $\{r^{(m)}\}=(r_1^{(m)}, r_2^{(m)}, ..., r_n^{(m)})^T$ due to unknown contact force $\{P^{(m)}\}=(P_1^{(m)}, P_2^{(m)}, ..., P_n^{(m)})^T$ is given as follows:

$$\left[C^{(m)}\right]\left\{P^{(m)}\right\}=\left\{r^{(m)}\right\} \tag{8}$$

Therefore, the following expressions, namely, the equilibrium equation and the condition ofcontact, are obtained:

$$\left.\begin{aligned} P_i^{(v)}+P_i^{(s)}&=0 \\ R_i^{(v)}+r_i^{(v)}&=R_i^{(s)}+r_i^{(s)} \end{aligned}\right\} \text{(contact)} \tag{9}$$

$$\left.\begin{aligned} P_i^{(v)}=P_i^{(s)}&=0 \\ R_i^{(v)}+r_i^{(v)}&>R_i^{(s)}+r_i^{(s)} \end{aligned}\right\} \text{(non}-\text{contact)} \tag{10}$$

where $R_i^{(s)}$ and $R_i^{(v)}$ denote the initial radii of the stent and the blood vessel, respectively, at i.

Then, by replacing $\{P^{(v)}\}$ and $-\{P^{(s)}\}$ with $\{P\}$, the equation of contact force is obtained as follows:

$$\left[C^{(v)}+C^{(s)}\right]\{P\}=\left\{R^{(s)}-R^{(v)}\right\} \tag{11}$$

Equation (11) is solved for $\{P\}$ to obtain the distribution of the contact force between the stent and the blood vessel wall. Since the rigidity of the strut section of the stent is considerably much lower than that of the wire section, $r_{ji}^{(s)}$ is negligible, except for the case in which i and j are located in the wire section of the stent. Therefore, in the present study, the influence matrix $[C^{(s)}]$ is composed by diagonally placing the partial matrix for the wire section, and the contact force on the strut section of the stent is not evaluated. The Gaussian elimination method is used to solve the simultaneous equations.

5.2 Calculation of distribution of straightening force on vascular wall

Straightening of the blood vessel occurs when a straight stent is inserted into a curved vessel. This insertion causes a straightening force to act on the vascular wall. The straightening effect should be evaluated while considering the interaction process of the expansion of the stent with the curved blood vessel. However, solving this problem is extremely complicated. Therefore, the straightening of the blood vessel is assumed to be independent from the expansion of the vessels by the stent, and it is simplified as shown in Fig. 12. The stent is approximated by a beam with the flexural rigidity obtained in the previous section, and the stent is modeled as a laminated beam by combining with a curved beam, which is used a model of the blood vessel.

The beam models are divided into n intervals. When a unit force is applied to point i of model m ($m = s, v$, which correspond to the stent and the vessel, respectively), the deflection at point j is denoted as $d_{ji}^{(m)}$. The n-order influence matrix $[D^{(m)}]$ is defined in terms of $d_{ji}^{(m)}$ as follows:

$$\left[D^{(m)}\right]=\left[\left\{d_1^{(m)}\right\},\left\{d_2^{(m)}\right\},\ldots,\left\{d_n^{(m)}\right\}\right] \tag{12}$$

where

$$\left\{d_i^{(m)}\right\}=\left(d_{1i}^{(m)},d_{2i}^{(m)},\ldots,d_{ni}^{(m)}\right)^{\mathrm{T}} \tag{13}$$

The force $\{F^{(m)}\}$ distributed along the beam is related to the deflection $\{d^{(m)}\}$ so as to satisfy the following equation:

$$\left[D^{(m)}\right]\left\{F^{(m)}\right\}=\left\{\delta^{(m)}\right\} \tag{14}$$

The equilibrium equation and contact condition are given by the following equations:

$$F_i^{(s)}+F_i^{(v)}=0 \tag{15}$$

$$\delta_i^{(s)}=\delta_i^{(i)}+\delta_i^{(v)} \tag{16}$$

where $d_i^{(i)}$ denotes the initial deflection of the blood vessel at point i, and $d_i^{(s)}$ and $d_i^{(v)}$ are the deflections of the stent and the blood vessel, respectively. Replacing -$\{F^{(v)}\}$ and $\{F^{(s)}\}$ with $\{F\}$, the equation of straightening force is obtained as follows:

$$\left[D^{(v)}+D^{(s)}\right]\{F\}=\left\{\delta^{(i)}\right\} \tag{17}$$

5.3 Limitations of these calculation methods

The methods will be useful for improving stent shape in order to reduce the peak force acting on the vascular wall. Although these methods are useful to calculate a contact force and a straightening force on a vascular wall, there are the following limitations:

1. The isotropic material property was assumed for the artery.
2. The cross-sectional distortions and thickness changes of the stent and blood vessel were ignored.
3. The friction on the contact surface between the stent and blood vessel was ignored.
4. It was consider that the straightening of the blood vessel and the expansion of the vessels by the stent were independent each other.
5. The stent and blood vessel were simplified by using axisymmetrical models in computation of the contact force and using the laminated beam in calculation of the straightening force, respectively.

6. Design method of stent suitable for diverse clinical manifestation

The stent must have the radial stiffness sufficient to expand the stenotic part in the blood vessel outward. Simultaneously, it must be sufficiently flexible to conform to the vascular wall. Neither the symptom nor the blood vessel shape is always in the same state. Therefore,

it is more important to design stents suited to each unique symptom of every patient. (Colombo et al., 2002) made evaluations of stent 'deliverability,' 'scaffolding,' 'accurate positioning,' and so on for the average lesion of the coronary artery. They proposed a guideline for use in determining a suitable stent. This guideline was based on clinical trials. Therefore, it is governed by the doctor's sense. One more noteworthy point is that the best-suited stent cannot be actually available for every specific symptom because a stent must be chosen only from among commercially available stents.

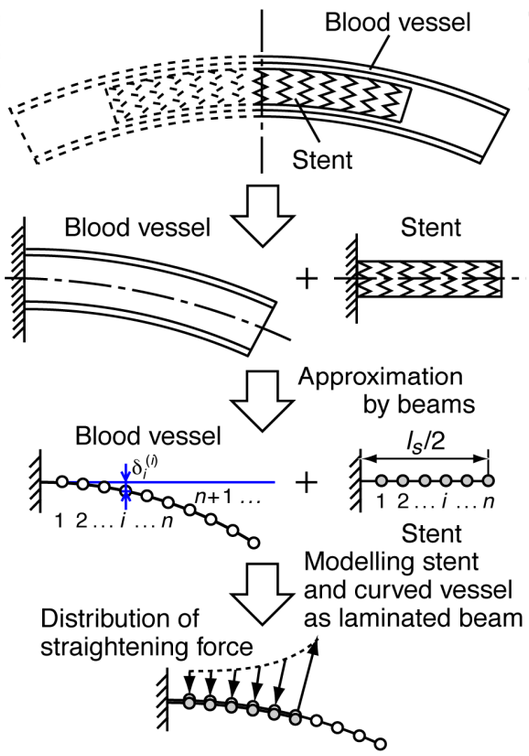

Fig. 12. Model for calculation of the straightening force on vascular wall. The stent andblood vessel are simply modeled as a laminated beam.

In this section, we describe a method for designing a stent that has good mechanical properties to suit diverse clinical manifestation. Figure 13 shows the flow of designing a stent suitable for diverse clinical manifestation. The first step is to determine the radial stiffness of the stent necessary to expand the stenotic part in the blood vessel based on symptom information. Next, based on the determined radial stiffness and the sensitivities of mechanical properties of the stent defined in Section 4, the design variables of a suitable stent are determined. In the second step, the force on the vascular wall by insertion of the designed stent is first evaluated by using the methods described in Section 5. This force is associated with the risk of in-stent restenosis. Next, based on the evaluation result, the designed stent is modified to be more suitable for the symptom. After modification, the force on the vascular wall is evaluated again. The effect of shape modification is confirmed by comparing the forces on the vascular wall between before and after modification. Finally, the modified stent shape is proposed as better suited stent shape. The detail of this proposed design method will be described in following sections.

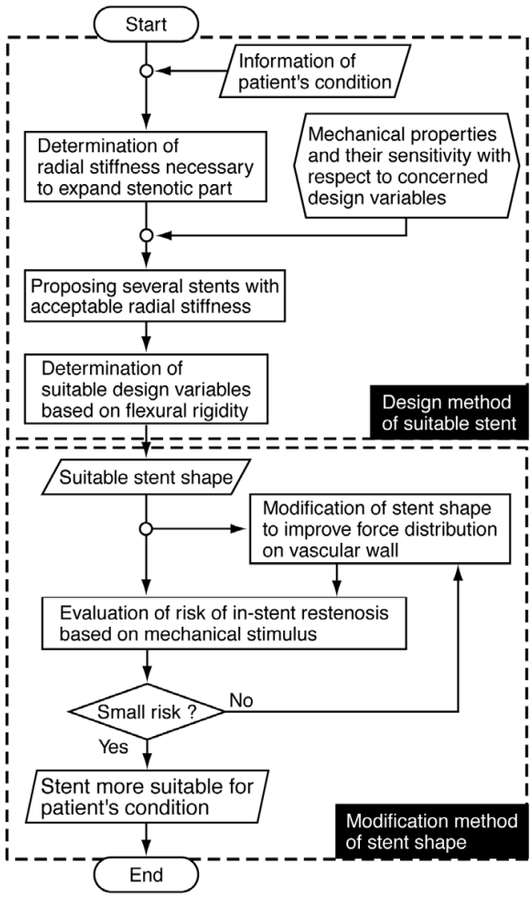

Fig. 13. Flow of designing stent suitable for diverse clinical manifestation. Designing a stent suitable for diverse clinical manifestation consists of two steps. In the first step, it is possible to design a stent necessary to expand the stenotic part of a blood vessel. In the second step, the designed stent is modified to suit the patient's symptom better.

6.1 Design method of stent having suitable mechanical properties to expand stenotic artery

6.1.1 Mechanical properties of artery model

When considering expanding the stenotic part in the blood vessel as presented in Fig. 14, it is important to know the vascular mechanical properties. Arteries in a living body are always pressured inside. Simultaneously, they are tensed with strain produced along its axial direction by several tens of percent. In this sense, it can be regarded as a thick cylinder being in a multiaxial stress state. It is necessary to assume such a multiaxial stress test to measure mechanical properties of the blood vessel. This means that it is extremely difficult to obtain mechanical properties of the blood vessel because the mechanical properties are associated with various levels and types of blood vessels.

In this study, the pressure strain elastic modulus propounded by (Peterson et al., 1960), which is easy to manipulate, is used. The pressure strain elastic modulus $E_{p,v}$ of a blood vessel can be expressed by the following equation

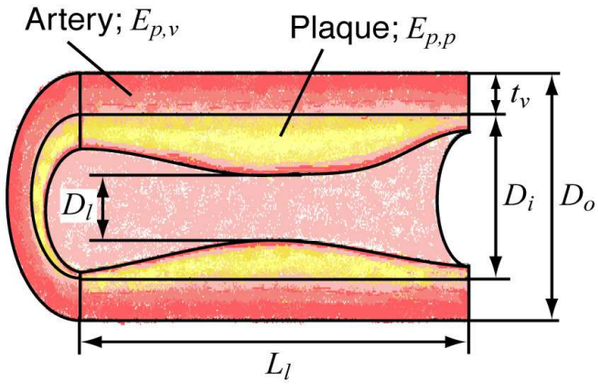

Fig. 14. Dimension of blood vessel with stenosis

$$E_{p,v} = \frac{\Delta p}{\Delta D_o / D_o} \tag{18}$$

where D_o is the blood vessel's outer diameter, and ΔD_o and Δp are the increase in the blood vessel diameter and the increase in the internal pressure respectively. The pressure strain elastic modulus has been used widely in clinical studies. Therefore, many reports on that subject are available. Table 3 presents value of the pressure strain elastic modulus for each type of human blood vessel, extracted from references (Hayashi et al., 1980; Hayashi, 2005; Stratouly et al., 1987; Gow & Hadfield, 1979), with modification.

Artery	$E_{p,v}$	Reporter
Arteria pulmonalis	0.016	Greenfield and Griggs (1963)
Ascending aorta	0.076	Patel et al. (1964)
Basilar artery	0.186 (β=14)	Hayashi et al. (1980)
Common carotid artery	0.049	Arndt et al. (1969)
Common iliac artery	0.120	Stratouly et al. (1987)
Coronary artery	0.602	Gow and Hadfield (1979)
Femoral artery	0.433	Patel et al. (1964)
Thoracic aorta	0.126	Luchsinger et al. (1962)

Table 3. Pressure strain elastic modulus for each type of human artery

6.1.2 Determination of radial stiffness necessary to expand stenotic part in artery

To determine the radial stiffness of the stent necessary to expand the stenotic part in the blood vessel, the requirements are, in addition to the pressure strain elastic modulus $E_{p,v}$ of the blood vessel, shown as follows. The outer and inner diameters, D_o and D_i, of the blood vessel in the normal state, the least diameter D_l produced by the stenotic part, and the length of the stenotic part L_l are required. The pressure strain elastic modulus of the plaque $E_{p,p}$ is required. Also required is the inner diameter after the treatment is made, D_t, which is an indicator to use as the target setting for the percentage by which to improve the blood flow level there. Given all the values listed above, the calculations for the necessary radial stiffness are made as follows.

By knowing that the increase in the blood vessel diameter is obtainable from circumferential strain of a cylinder, the blood vessel with stenosis can be modeled by simply using springs connected in parallel, as presented in Fig. 15. Thus, the internal pressure in blood vessel p^*,

which is necessary to expand the stenotic part, can be obtained by

$$p^* = \left(E_{p,v} + E_{p,p}\right)\frac{D_t - D_l}{D_o} = E_{p,vl}\frac{D_t - D_l}{D_o} \tag{19}$$

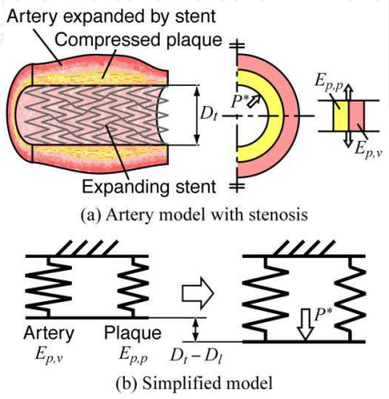

Fig. 15. Simplified modeling of expansion of stenosis in artery by insertion of stent

When measuring the pressure strain elastic modulus of the plaque $E_{p,p}$ is difficult, it is possible to replace the sum of the elastic moduli, $E_{p,v}$ + $E_{p,p}$, by the pressure strain elastic modulus of the diseased blood vessel $E_{p,vl}$, which can be easily measured.

As a matter of fact, the diameter of the stent, which is inserted into the stenotic part, is greater than the target vascular diameter after treatment. In conclusion, from the stent diameter d_s and the target vascular diameter D_t obtained after treatment, the radius reduction Δr in stent after inserting can be calculated by means of the following equation:

$$\Delta r = \frac{d_s - D_t}{2} \tag{20}$$

By substituting equations (19) and (20) into $K_p = p/\Delta r$, which was defined by (Yoshino et al., 2008) to obtain the radial stiffness, the radial stiffness K_p necessary to expand the stenotic part can be obtained from

$$K_p^* = 2\left(E_{p,v} + E_{p,p}\right)\frac{D_t - D_l}{D_o\left(d_s - D_t\right)} = 2E_{p,vl}\frac{D_t - D_l}{D_o\left(d_s - D_t\right)} \tag{21}$$

The obtained K_p^* is the least required stiffness to expand the stenotic part in the blood vessel. Therefore, when designing a stent, the chosen stiffness should be greater than this K_p^* value.

Now consider the case where a stent with a diameter of 6 mm is inserted into a coronary artery. The symptoms shown in Table 4 are examples based on references (Gow & Hadfield, 1979; Le Floc'h et al., 2009). Based on this data, the radial stiffness K_p^* necessary to expand the stenotic part in the blood vessel is calculated by equation (21) to be K_p^* = 366.7 MPa/m.

The required radial stiffness K_p^* is plotted as a broken line on the radial stiffness map shown in Fig. 16. From this line, it is possible to determine the design variables for a stent with sufficient radial stiffness to expand the stenotic part of the blood vessel. Based on these, the designer can proceed to work with some design propositions.

Coronary artery	Parameters
Outer diameter, D_o (mm)	4.90
Inner diameter, D_i (mm)	4.06
Least diameter of lesion, D_l (mm)	2.5
Length of lesion, L_l (mm)	10
Total flexion angle (deg.) (Flexion angle (deg.))	90 (45)
Rate of stenosis by ECST method (%)	38.4
Pressure strain elastic modulus of artery, $E_{p,v}$ (MPa)	0.602
Pressure strain elastic modulus of diseased artery, $E_{p,vl}$ (MPa)	0.628
Inner diameter after treatment, D_t (mm)	4.56

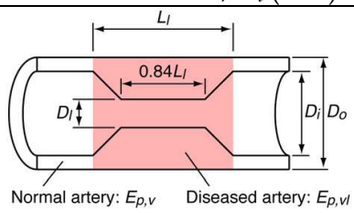

Schematic view of assumed symptom

Table 4. Assumed patient symptom information

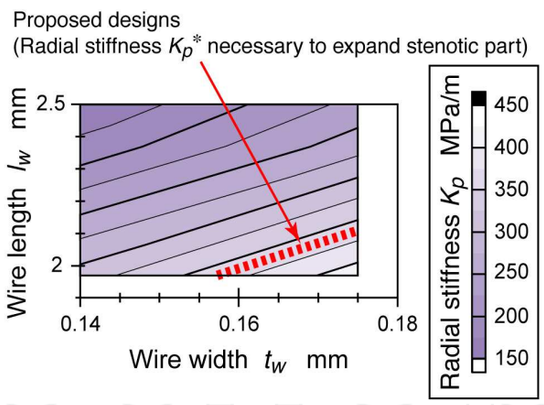

Fig. 16. Proposed designs having the radial stiffness necessary to expand the stenotic part of a blood vessel. By assuming that a stent is inserted into a coronary artery, a value of 0.602 MPa was used for the pressure strain elastic modulus $E_{p,v}$ of the normal part of the coronary artery, and a value of 0.628 MPa for the pressure strain elastic modulus $E_{p,vl}$ of the diseased artery. For the coronary artery model, D_o = 4.90 mm, D_i = 4.06 mm, and D_l = 2.5 mm were assumed. The corresponding part of the map is magnified and displayed.

6.1.3 Range of selectable flexural rigidity and the dilemma of selecting the design

After inserting an originally straight stent into a curved blood vessel and leaving it there, the stent generally conforms to the blood vessel shape. Nevertheless, because the flexural

rigidity of the stent is greater than that of the blood vessel, the blood vessel tends to become straighter. This phenomenon of straightening of the blood vessel was previously described in detail, and a method to calculate the force resulting in the straightening of the blood vessel was described in previous section. It is apparent that this force depends on the flexural rigidity of the stent, and that greater flexural rigidity results in a larger force. A force too large can damage the vascular wall. Consequently, it is important to choose the most appropriate flexural rigidity of the stent.

By plotting the proposed designs obtained from the required radial stiffness K_p^* on a flexural rigidity map, the broken line shown in Fig. 17(a) is obtained. For one radial stiffness value, multiple flexural rigidity values can be selected as long as they are within the range given in the figure. None of the limiting values for the flexural rigidity, which might prevent damage on the vascular wall or neointimal thickening, are yet quantitatively available. Therefore, the flexural rigidity should be made smaller to decrease the force acting on the vascular wall. In other words, the designer should select the smallest flexural rigidity from the range of selectable values shown in Fig. 17(a).

Figure 17(b) shows the stent shape designed in consideration of the rules described above. The designed stent is referred to as SDCO and has a wire length l_w^* of 2.01 mm, and a wire width t_w^* of 0.16 mm. In addition, the length of the designed stent is determined so that it occupies the blood vessel from the stenotic part to the normal part at each end in consideration of actual clinical use. The length of the SDCO is 22.0 mm (the stent consists of 8 wire sections and 7 strut sections). The flexural rigidity of the SDCO is $K_b^* = 25.1 \times 10^{-6}$ Nm^2. Similarly, the shear rigidity of the SDCO, based on the map of the rigidity, is $K_s^* = 1.33$ N.

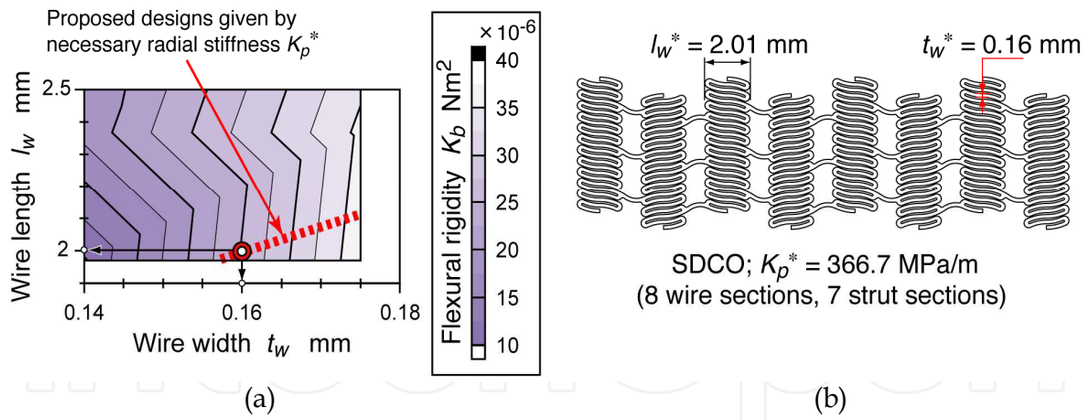

Fig. 17. Selection of the proposed design from the viewpoint of flexural rigidity. (a) The selectable range of flexural rigidities is indicated by the broken line. The corresponding part of the map is magnified and displayed as in Fig. 16. (b) A stent 6 mm in diameter is designed to suit the assumed symptom of the coronary artery.

6.2 Evaluation of the risk of in-stent restenosis based on the mechanical stimulus

Figure 18 shows the distributions of the contact force and the straightening force when the SDCO is inserted into the coronary artery. These distributions were calculated by the previously described method, which was proposed by (Yoshino et al., 2011).

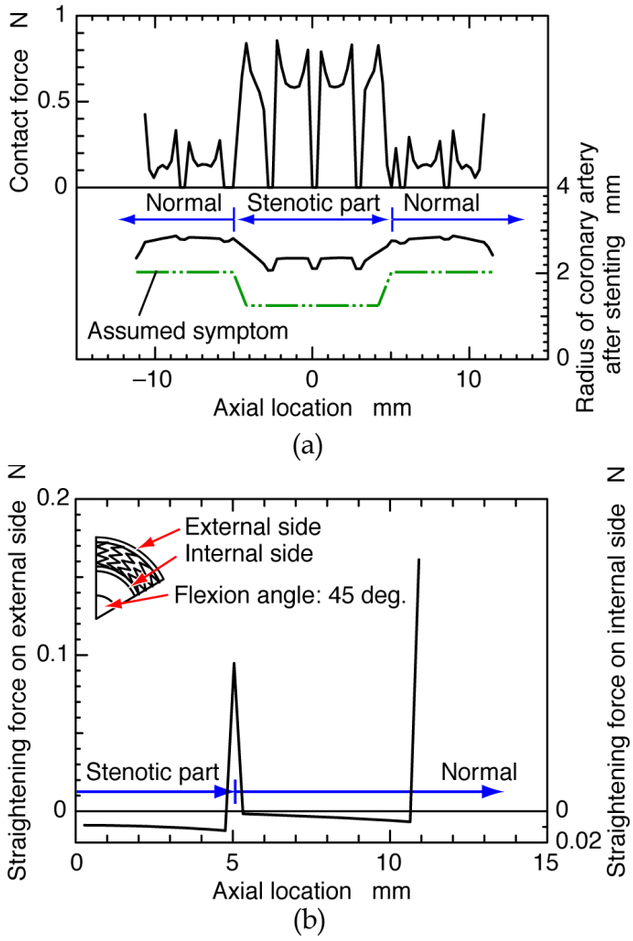

Fig. 18. Computational results of forces which are exerted on the coronary artery wall by insertion of the SDCO. (a) The distribution of the contact force between the SDCO and the coronary artery (upside), and the radius of the coronary artery after stenting (downside). The dot-dashed line indicates the initial shape of the artery wall with the assumed symptom. (b) The distribution of the straightening force on the coronary artery wall by insertion of the SDCO. The right side of the distribution is displayed from a consideration of the geometrical symmetry.

First, let us focus attention on the force on the vascular wall. Although the contact force is large at the stenotic part, the generation of this large force is unavoidable for expansion of the stenotic part. The contact force is also concentrated at both ends of the stent. The straightening force on the vascular wall is concentrated at the end of the stenotic part in addition to both ends of the stent.

It has been reported that the hyperplasia of smooth muscle cells and the neointimal proliferation occur at the stented part of an artery (Grewe et al., 2000; Clark et al., 2006). It is assumed that the hyperplasia and proliferation are caused by the mechanical stimulus acting on the vascular wall due to insertion of the stent. (Schweiger et al., 2006) reported that

in-stent restenosis occurred primarily at both ends of the stent during the period one to three months after stenting. In the study of (Lal et al., 2007), the majority of patients in the target patient population showed in-stent restenosis at the stent ends. (Yazdani and Berry, 2009) cultured a stented native porcine carotid artery under physiologic pulsatile flow and pressure conditions for a week. They confirmed that the proliferation of smooth muscle cells occurred significantly at both ends of the stent. By summarizing these reports and evaluation results of the forces on the vascular wall, it is concluded that the force concentration provokes neointimal thickening due to the hyperplasia of smooth muscle cells, i.e., in-stent restenosis.

Next, the expansion of the vascular wall is examined. The normal part of the artery is expanded to become much larger than the target diameter. This excessive expansion causes expansion of the entire stented part. As a result, stagnation and vortices of blood flow are induced, further increasing the potential for stent thrombosis.

The designed stent has mechanical properties sufficient to expand the stenotic part of theartery, but is not suitable for the normal part of the artery. Thus, it requires modification.

6.3 Effective method to modify the stent shape in consideration of the risk of in-stent restenosis

6.3.1 Design objective for the shape modification

In the previous section, it was shown that although a stent suitable for the assumed symptoms could be designed using the proposed design method, further modifications were still required. Two kinds of design objectives are set up for shape modification.

Objective for the mechanical stimulus: as shown in Fig. 18, the contact force on the normal part of the artery is concentrated at both ends of the stent. This force concentration provokes neointimal thickening from the hyperplasia of smooth muscle cells. Therefore, the contact force must be reduced at both ends of the stent. However, this force should be larger than a certain limit so that stent functions on the lesion.

Objective for the blood flow: as stated above, the normal part of the artery is expanded to become much larger than the target diameter. This expansion state of the artery causes stagnation and vortices of blood flow. As a result, stent thrombosis may be induced. It is very important to reduce stagnation and vortex creation to decrease the risk of stent thrombosis. Therefore, the vascular wall should be expanded flatly by the insertion of the stent. The flat expansion of the artery can prevent the generation of stagnation and vortices in the stented artery.

6.3.2 Modification method of the stent shape to suit the clinical manifestation

The stent designed in the previous section has a uniform radial stiffness K_p^* along its axial direction. The radial stiffness K_p^* causes excessive expansion at the normal part of the artery because K_p^* was calculated for expansion of the stenotic part, which is generally stiffer than the normal part. The objective for the mechanical stimulus can be attained by decreasing the radial stiffness to a value corresponding to that of a normal artery. At the same time, the

objective for blood flow must be attained. Therefore, the stent should have a radial stiffness K_p^{**} to expand the vascular wall at normal part only for the stent thickness t. This can achieve the flat expansion of the artery. By changing the stent radial stiffness at the normal part from K_p^{*} to K_p^{**} , the contact force can also decrease. In this study, it was decided to adopt the radial stiffness K_p^{**} as a compromise between the two design objectives.

The methods using the influence matrix described in Section 5 are used for the shape modification. Figure 19 shows the concept for modification of the stent shape. The distributed contact force P_i^* on the stenotic part can be calculated based on the radial stiffness K_p^*, as follows:

$$P_i^* = \frac{\pi D_t K_p^* \Delta r_t l_w^*}{n_{\mathrm{CP}}} \tag{22}$$

where D_t is the inner diameter of the blood vessel after treatment, Δr_t is the increase in the vascular radius of the target, l_w^* is the wire length of the stent designed based on the radial stiffness K_p^*. Also, n_{CP} represents the number of calculation points on the wire section. For simplicity, it was assumed that a uniform contact force was exerted on the vascular wall.

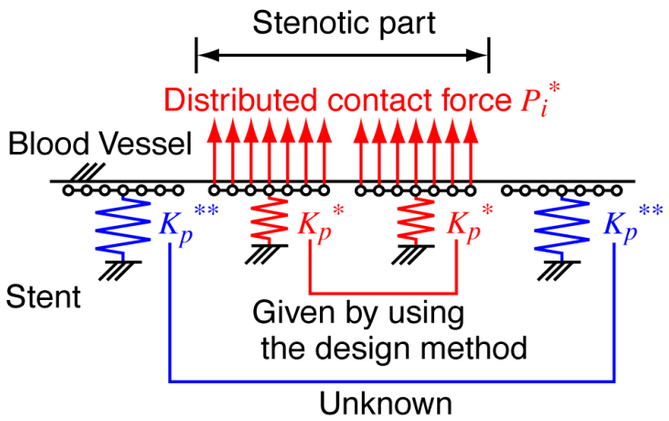

Fig. 19. Concept for modification of the stent shape. The distributed contact force is obtained from the radial stiffness of the stent on the stenotic part by using the design method. The force that should be applied on the normal artery is calculated by using the obtained distributed contact force on the stenotic part.

As described in Section 5, the radial displacement of the vascular wall $\{r^{(v)}\} = (r_1^{(v)}, r_2^{(v)}, \ldots, r_n^{(v)})^{\mathrm{T}}$ due to the unknown contact force $\{P\} = (P_1, P_2, \ldots, P_n)^{\mathrm{T}}$ is given as follows:

$$\left[C^{(v)}\right]\{P\} = \left\{r^{(v)}\right\} \tag{23}$$

where $[C^{(v)}]$ is the influence matrix of the blood vessel, defined by the radial displacement of the vascular wall due to the unit radial force. The calculated contact force P_i^* is substituted

into equation (23), and the influence matrix $[C^{(v)}]$ is downsized to the matrix $[C_{\text{normal}}{}^{(v)}]$ of the normal blood vessel.

$$\left[C_{\text{normal}}^{(\text{v})}\right]\left\{P^{**}\right\}=\left\{r_{\text{normal}}^{(\text{v})}\right\}+\left[C_{\text{stenosis}}^{(\text{v})}\right]\left\{P^{*}\right\} \tag{24}$$

$[C_{\text{stenosis}}{}^{(v)}]$ is the influence matrix of the stenotic part, and $\{r_{\text{normal}}{}^{(v)}\}$ is the radial displacement of the normal part of the blood vessel wall. Equation (24) is solved for $\{P^{**}\}$ to obtain the distributed force P_i^{**} that can expand the normal part to the stent thickness t.

Here, it is assumed that the wire length after modification is l_w^{**} and the calculation points from k to l are included in the modified wire section. The required radial stiffness K_p^{**} is defined as follows:

$$K_p^{**}=\frac{\sum_{i=k}^{l}P_i^{**}}{\pi D_t l_w^{**} t} \tag{25}$$

The K_p^{**} value calculated by equation (25) is plotted on the radial stiffness map. As a result, the wire width t_w^{**} after modification is determined from the l_w^{**} value and the curve of K_p^{**} on the map. Therefore, the designed stent has to be modified to the shape of l_w^{**} and t_w^{**} at the normal part of the blood vessel. Considering that an increase in the stent length is undesirable, the designer should keep the wire length l_w^{**} equal to l_w^{**} after the modification. However, it is possible that the wire width t_w^{**} after the modification cannot be obtained because of the mismatch between the assumed l_w** value and the curve of K_p^{**}. In this case, the designer can increase the wire length l_w** , perform the same procedures, and determine the l_w^{**} and t_w^{**} values.

The required radial stiffness K_{p1}^{**} at both ends of the SDCO is 50.3 MPa/m. The radial stiffness K_{p2}^{**} at the normal part of the artery except for both stent ends is also calculated as 155.2 MPa/m. From the dot-dashed curves of K_{p1}^{**} and K_{p2}^{**} shown in Fig. 20(a), it is determined that l_{w1}^{**} is 2.52 mm, t_{w1}^{**} is 0.087 mm, l_{w2}^{**} is 2.01 mm, and t_{w2}^{**} is 0.094 mm. Figure 20(b) shows the modified shape of the SDCO.

The flexural rigidity K_{b1}^{**} at both ends of the SDCO is 5.75×10^{-6} Nm^2, and the shear rigidity K_{s1}^{**} is 0.20 N. At the normal part of the artery except for both stent ends, the flexural rigidity K_{b2}^{**} of the SDCO is 6.00×10^{-6} Nm^2, and the shear rigidity K_{s2}^{**} is 0.42 N.

6.3.3 Confirmation of the effect of the shape modification

Figure 21 shows a comparison of the force on the vascular wall by insertion of the stent before and after the modifications. After the modifications of the SDCO, an approximately 80 % reduction in the concentrated contact force was attained (Fig. 21(a)). Furthermore. the concentrated straightening force at the stent ends after modification was reduced to approximately 35 % of that before modification of the SDCO (Fig. 21(b)).

On the other hand, it is recognized that straightening force increases at the stenotic-healthy tissue interface (the axial location is 5 mm in Fig. 21(b)). The concentration of straightening force also occurs at the axial location of 8 mm. After modification of the stent shape, the flexural and shear rigidities of the stent vary with the axial location. The bending state of the stent changes at the changing point of the rigidities, which corresponds to the turn of the stent shape. Therefore, straightening force increases due to changing of the stent bending state based on rigidities changing. Although the risk of the vessel rupture slightly increases at the stenotic-healthy tissue interface, it is achieved that the straightening force is significantly reduced at both ends of the stent, where the hyperplasia of smooth muscle cells is frequently reported.

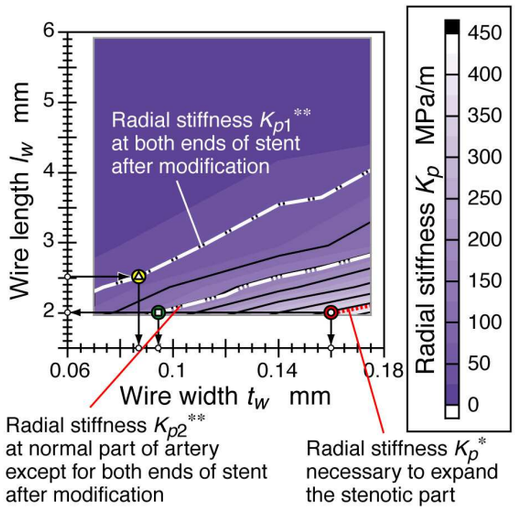

(a)

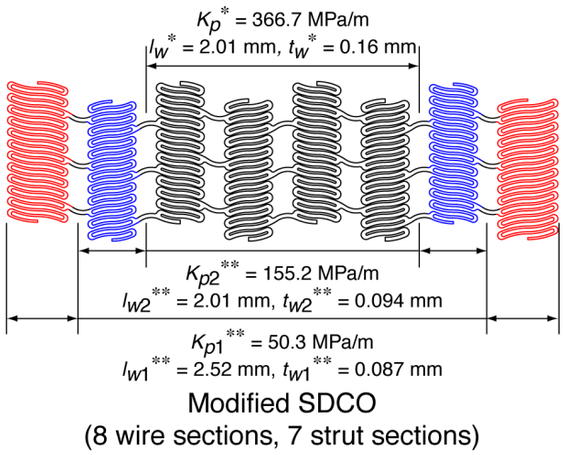

(b)

Fig. 20. The SDCO stent 6 mm in diameter is modified to suit the assumed symptom of the coronary artery. (a) Design variables after modification are determined by using the map of the radial stiffness. (b) The modified SDCO has a nonuniform shape along its axial direction.

The modified stent can expand the vascular wall in a more flat manner. Therefore, modification of the designed stent by using the proposed method can relax the force concentration at both ends of the stent by attaining flat expansion of the vascular wall.

7. Conclusion

This chapter described evaluating mechanical properties of a stent and designing/selecting a stent suitable for diverse clinical manifestation by efficiently using the evaluated results. By rounding up the results described above, it can be confirmed that two objectives, which are establishments of designing/selecting a stent suitable for diverse clinical manifestation, were achieved. The stent, which is designed by using the method described in this chapter, has nonuniform shapes along its axial direction. This shape is radically new compared to the conventional stent shape that is uniform along its axial direction. Thus, the stent shape designed by using the method is considered to be a new-generation type.

8. References

Babapulle, M. N.; Joseph, L., Bélisle, P., Brophy, J. M., & Eisenberg, M. J. (2004). A hierarchical Bayesian meta-analysis of randomised clinical trials of drug-eluting stents. *Lancet*, Vol. 364, No. 9434, (August 2004) 583-591, ISSN 0140-6736 (print version).

Carnelli, D.; Pennati, G., Villa, T., Baglioni, L., Reimers, B., & Migliavacca, F. (2010). Mechanical properties of open-cell, self-expandable shape memory alloy carotid stents. *Artificial Organs*, Vol. 35, No. 1, (January 2011) 74-80, ISSN 0160-564X (print version).

Clark, D. J.; Lessio, S., O'Donoghue, M., Tsalamandris, C., Schainfeld, R., & Rosenfield, K. (2006). Mechanisms and predictors of carotid artery stent restenosis--A serial intravascular ultrasound study. *Journal of the American College of Cardiology*, Vol. 47, No. 12, (June 2006) 2390-2396, ISSN 0735-1097.

Colombo, A.; Stanlovic, G., & Moses, J. W. (2002). Selection of coronary stents. *Journal of the American College of Cardiology*, Vol. 40, No. 6, (September 2002) 1021-1033, ISSN 0735-1097.

Duda, S. H.; Wiskirchen, J. Tepe, G., Bitzer, M., Kaulich, T. W., Stoeckel, D., & Claussen, C. D. (2000). Physical properties of endovascular stents: an experimental comparison. *Journal of Vascular and Interventional Radiology*, Vol. 11, No. 5, (May 2000) 645-654, ISSN 1051-0443.

Gow, B. S. & Hadfield C. D. (1979). The elasticity of canine and human coronary arteries with reference to postmortem changes. *Circulation Research*, Vol. 45, No. 5, (November 1979) 588-594, ISSN 0009-7330.

Grewe, P. H.; Deneke, T., Machraoui, A., Barmeyer, J., & Müller, K.-M. (2000). Acute and chronic tissue response to coronary stent implantation: pathologic findings in human specimen. *Journal of the American College of Cardiology*, Vol. 35, No. 1, (January 2000) 157-163, ISSN 0735-1097.

Hayashi, K. (2005). *Biomechanics*, Corona Publishing, Tokyo, Japan. (in Japanese)

Hayashi, K.; Handa, H., Nagasawa, S., Okumura, A., & Moritake, K. (1980). Stiffness and elastic behavior of human intracranial and extracranial arteries. *Journal of Biomechanics*, Vol. 13, No. 2, 175-184, ISSN 0021-9290.

Kastrati, A.; Mehilli, J., Pache, J., Kaiser, C., Valgimigli, M., Kelbaek, H., Menichelli, M., Sabaté, M., Suttorp, M. J., Baumgart, D., Seyfarth, M., Pfisterer, M. E., & Schömig, A. (2007). Analysis of 14 trials comparing sirolimus-eluting stents with bare-metal stents. *The New England Journal of Medicine*, Vol. 356, No.10, (March 2007) 1030-1039, ISSN 0028-4793 (print version).

Lagerqvist, B.; James, S. K., Stenestrand, U., Lindbäck, J., Nilsson, T., & Wallentin, L. (2007). Long-term outcomes with drug-eluting stents versus bare-metal stents in Sweden. *The New England Journal of Medicine*, Vol. 356, No. 10, (March 2007) 1009-1019, ISSN 0028-4793 (print version).

Lal, B. K.; Kaperonis, E. A., Cuadra, S., Kapadia, I., & Hobson, R. W. 2nd. (2007). Patterns of in-stent restenosis after carotid artery stenting: classification and implications for long-term outcome. *Journal of Vascular Surgery*, Vol. 46, No. 5, (November 2007) 833-840, ISSN 0741-5214.

Le Floc'h, S.; Ohayon, J., Tracqui, P., Finet, G., Gharib, A. M., Maurice, R. L., Cloutier, G., & Pettigrew, R. I. (2009). Vulnerable atherosclerotic plaque elasticity reconstruction based on a segmentation-driven optimization procedure using strain measurements: theoretical framework. IEEE transactions on medical imaging. Vol. 28, No. 7, (July 2009) 1126-1137, ISSN 0278-0062.

Mori, K. & Saito, T. (2005). Effects of stent structure on stent flexibility measurements. *Annals of Biomedical Engineering*, Vol. 33, No. 6, (June 2005) 733-742, ISSN 0090-6964 (print version).

Morice, M.-C.; Serruys, P. W., Sousa, J. E., Fajadet, J., Hayashi, E. B., Perin, M., Colombo, A., Schuler, G., Barragan, P., Guagliumi, G., Molnar, F., & Falotico, R. (2002) A randomized comparison of a sirolimus-eluting stent with a standard stent for coronary revascularization. *The New England Journal of Medicine*, Vol. 346, No. 23, (June 2002) 1773-1780, ISSN 0028-4793 (print version).

Nordmann, A. J.; Briel, M., & Bucher, H. C. (2006). Mortality in randomized controlled trials comparing drug eluting vs. bare metal stents in coronary artery disease: a meta-analysis. *European Heart Journal*, Vol. 27, No. 23, (December 2006) 2784-2814, ISSN 0195-668X (print version).

Peterson, L. H.; Jensen, R. E., & Parnell, J. (1960). Mechanical properties of arteries in vivo. *Circulation Research*, Vol. 8, No. 3, (May 1960) 622-639, ISSN 0009-7330.

Schweiger, M. J.; Ansari, E., Giugliano, G. R., Mathew, J., Islam, A., Morrison, J., & Cook, J. R. (2006). Morphology and location of restenosis following bare metal coronary stenting. *The Journal of Invasive Cardiology*, Vol. 18, No. 4, (April 2006) 165-168, ISSN 1042-3931.

Stratouly, L. I.; Cardullo, P. A., Anderson, F. A. Jr., Durgin, W. W., & Wheeler, H. B. (1987). The use of ultrasound imaging in the in-vivo determination of normal human arterial compliance. *Proceedings of the 13th Annual Northeast Bioengineering Conference*, pp.435-437, Philadelphia, PA, U.S., March 1987, Defense Technical Information Center, Fort Belvoir.

Tamakawa, N.; Sakai, H., & Nishimura, Y. (2008). Prediction of restenosis progression after carotid artery stenting using virtual histology IVUS. *Journal of Neuroendovascular Therapy*, Vol. 2, No. 3, (December 2008) 193-200, ISSN 1882-4072.

Yazdani, S. K. & Berry, J. L. (2009). Development of an in vitro system to assess stent-induced smooth muscle cell proliferation: a feasibility study. *Journal of Vascular and Interventional Radiology*, Vol. 20, No. 1, (January 2009) 101-106, ISSN 1535-7732.

Yoshino, D. & Inoue, K. (2010). Design method of self-expanding stents suitable for the patient's condition. *Proceedings of the Institution of Mechanical Engineers, Part H: Journal of Engineering in Medicine*, Vol. 224, No. 9, (September 2010) 1019-1038, ISSN 0954-4119 (print version).

Yoshino, D.; Inoue, K., & Narita, Y. (2008) Mechanical properties of self-expandable stents: a key to product design of suitable stents. *Proceedings of the 7th International Symposium on Tools and Methods of Competitive Engineering*, Vol. 1, pp. 659-672, ISBN 978-90-5155-044-3, Izmir, Turkey, April 2008.

Yoshino, D.; M. Sato, & K. Inoue. (2011). Estimation of force on vascular wall caused by insertion of self-expanding stents. *Proceedings of the Institution of Mechanical Engineers, Part H: Journal of Engineering in Medicine*, Vol. 224, No. 8, (August 2011) 831-842, ISSN 0954-4119 (print version).

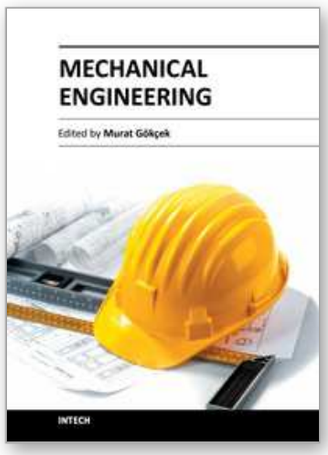

Mechanical Engineering

Edited by Dr. Murat Gokcek

ISBN 978-953-51-0505-3
Hard cover, 670 pages
Publisher InTech
Published online 11, April, 2012
Published in print edition April, 2012

The book substantially offers the latest progresses about the important topics of the "Mechanical Engineering" to readers. It includes twenty-eight excellent studies prepared using state-of-art methodologies by professional researchers from different countries. The sections in the book comprise of the following titles: power transmission system, manufacturing processes and system analysis, thermo-fluid systems, simulations and computer applications, and new approaches in mechanical engineering education and organization systems.

InTech Europe
University Campus STeP Ri
Slavka Krautzeka 83/A
51000 Rijeka, Croatia
Phone: +385 (51) 770 447
Fax: +385 (51) 686 166
www.intechopen.com

InTech China
Unit 405, Office Block, Hotel Equatorial Shanghai
No.65, Yan An Road (West), Shanghai, 200040, China
中国上海市延安西路65号上海国际贵都大饭店办公楼405单元
Phone: +86-21-62489820
Fax: +86-21-62489821

IntechOpen